Available online at www.sciencedirect.com
SCIENCE DIRECT®
European Journal of Pharmaceutics and Biopharmaceutics 57 (2004) 431–439
European Journal of Pharmaceutics and Biopharmaceutics
www.elsevier.com/locate/ejpb

Research paper

The assessment of the relaxation behaviour of frozen aqueous solutions of human serum albumin and polyvinylpyrrolidine

Susan A. Barker*

School of Chemical Sciences and Pharmacy, University of East Anglia, Norwich, UK

Received 8 October 2003; accepted in revised form 24 February 2004

Abstract

In this investigation, the structure and behaviour of frozen solutions of human serum albumin (HSA) alone and in combination with the cryoprotectant polyvinylpyrrolidone (PVP) have been studied using low frequency dielectric analysis and modulated temperature differential scanning calorimetry (MTDSC). Solutions of HSA (1–10 w/v%) and combined solutions (from 1 to 5 w/v% of each ingredient) were prepared and studied thermally and dielectrically over a frequency range of 10^5–10^{-2} Hz every 10 °C from +20 to −70 °C. Dielectric data were fitted according to the Dissado–Hill theory and the relaxation times calculated. In addition, a relaxation peak was noted for the frozen HSA systems at a frequency approximately one order of magnitude lower than that seen for the PVP systems, with the PVP dominating the response of the mixed systems. The systems showed Arrhenius behaviour, with, for example, the 5% HSA solution showing an activation energy for the relaxation process of 19.34 kJ/mol. In accordance with previous studies on frozen aqueous solutions of PVP, the results suggest that unfrozen water dominated the dielectric response, with the local environment surrounding the HSA being strongly influenced by the PVP. MTDSC data indicated that the PVP and HSA interact in a complex manner in solution, with a glass transition attributable to PVP being seen only in those systems where PVP was present in sufficient excess. In conclusion, the study has suggested that MTDSC and dielectric spectroscopy may be the useful complementary tools with which the structure and molecular mobility of frozen proteinaceous systems may be studied.

Keywords: Human serum albumin; Polyvinylpyrrolidone; Dielectric spectroscopy; Relaxation; Modulated temperature differential scanning calorimetry; Frozen; Solution

1. Introduction

The increasing utilisation of freeze-drying production protocols within the pharmaceutical industry, generally in order to improve the stability of labile products, has necessitated the investigation of this method from a physicochemical standpoint. In particular, there is a recognised need to understand the structure of the material in question at all stages of the freeze-drying process, particularly in the context of investigating the role of cryo- and lyoprotectants in preserving the integrity of pharmaceutical proteins during and after the freeze-drying process. There are several excellent reviews in the literature, which give an overview of the uses of freeze-drying technology [1–3].

The first stage in the freeze-drying process is the formation of an aqueous solution consisting of the active pharmaceutical ingredient, typically a protein or peptide, and formulation adjuvants, such as bulking agents, tonicity modifiers, pH modifiers and cryoprotectants [2]. The temperature of the solution is then reduced to below 0 °C, allowing the formation of ice crystals, and hence, by effective removal of water from the system, an increase in solute concentration. For the majority of mono-component solutions, the remaining liquid ultimately attains a maximum concentration of solute C'_g and undergoes a glass transition at a characteristic temperature T'_g [4]. For multi-component solutions, the situation is obviously more complex, with the possibility of at least partial precipitation of individual constituents once their solubility limits have been reached, or the separation of the system into multiple phases, each

* Address: School of Chemical Sciences and Pharmacy, University of East Anglia, Norwich NR4 7TJ, UK. Tel.: +44-1603-592843; fax: +44-1603-592003.
E-mail address: susan.barker@uea.ac.uk (S.A. Barker).

0939-6411/$ - see front matter © 2004 Elsevier B.V. All rights reserved.
doi:10.1016/j.ejpb.2004.02.009

containing one or more components. In both these situations, the stabilising influence of the excipient may be lost, leading to possible protein degradation or denaturation during subsequent processing or storage. It has been suggested that for optimum stability of the final product, a 'single-phase glass' containing the protein and all required excipients must be formed at this stage [5]. It is extremely helpful, therefore, to have a full understanding of the nature of this initial frozen system, in terms of its structure, i.e. single phase or multiple excluded phases, and its glass transitional behaviour, which will determine subsequent processing conditions and likely stability issues.

In addition, it has been suggested that knowledge of the relaxation behaviour of amorphous systems above and below their T_g can be used to predict the physical and chemical stability of such systems [6,7]. Recently, there has been considerable interest in the development of means by which the relaxation time may be assessed, with techniques such as differential scanning calorimetry (DSC) [8] and rheology [9] having been studied. There are, however, two main issues common to all techniques used in this mode: (a) the timescales on which molecular motions and relaxations occur below the T_g are long and generally outside the experimental time window available; and (b) low temperatures are required to adequately study the frozen systems encountered during freeze-drying protocols, which may lead to experimental difficulties. These, taken together with the difficulty of extrapolating information gained above the T_g to temperatures below the T_g, have lead to the development of mathematical predictions of sub-T_g relaxation times, such as that of Shamblin et al. [7]. There is nevertheless a need for a simple, quick technique which will measure the relaxation time of sub-T_g amorphous systems directly.

One area of study which warrants further investigation is the state of the water within the frozen aqueous system as it is known that there is an association between the non-frozen water of the system and the stability of proteins during the freeze-drying process [3,10]. Several authors have used nuclear magnetic resonance (NMR) spectroscopy to study the distribution and mobility of water within complex samples. For example, Okada et al. [11] studied the mobility of water in frozen pullulan aqueous solutions, concluding that non-frozen water was present in the frozen systems, and Le Botlan et al. [12] studied the state of water and oil in frozen simple emulsions, determining that approximately 99% of the water in these systems was present as ice. Barker et al. [13] showed that low frequency dielectric spectroscopy could be used to examine frozen aqueous solutions of the cryoprotectant polyvinylpyrrolidone (PVP), identifying a relaxation peak in the dielectric loss due to the non-frozen water in the system. The data indicated that the water in the maximally freeze-concentrated solutions existed in an area of high local viscosity, giving rise to a relatively long relaxation time of circa 100 μs, and that the relaxation process followed Arrhenius kinetics, with an activation energy of circa 12 kJ/mol. Modulated temperature differential scanning calorimetry (MTDSC) of these solutions showed a small but reproducible glass transition at circa −19 °C, indicating that the systems were in the sub-T'_g temperature range for all of the dielectric spectroscopy studies. Thus, the relaxation behaviour of non-frozen water in these systems below their T'_g could be studied directly.

In the present study, these investigations have been extended to include the examination of frozen aqueous solutions of a model protein, human serum albumin (HSA), and mixed solutions of the cryoprotectant and the protein by low frequency dielectric spectroscopy and MTDSC. In this manner, it is intended that a greater understanding of the structure of a multi-component frozen system may be obtained and the technique of low frequency dielectric spectroscopy developed as a useful tool for freeze-drying applications.

2. Dielectric spectroscopy

Dielectric spectroscopy is an electrical technique, whereby an alternating voltage of varying frequency is applied to a sample. A polarisation current is generated in response to this applied voltage via the reorientation of any dipoles, either permanent or induced, present within the sample. The complex polarisation current is then deconvoluted into the in-phase (imaginary) and out-of-phase (real) components, these being measures of the energy lost from and stored within the system, respectively. Mathematically, the response of the sample is described by the complex permittivity ε^* at an angular frequency ω which is expressed in terms of the real and imaginary components:

$$\varepsilon^*(\omega) = \varepsilon'(\omega) - \mathrm{i}\varepsilon''(\omega) \tag{1}$$

The real and imaginary permittivities are derived from the experimentally determined capacitance C and dielectric loss $G(\omega)/\omega$, where G is the conductance of the system at frequency ω. The real part of the permittivity $\varepsilon'(\omega)$ is related to the measured capacitance C at frequency ω by

$$C(\omega) = \frac{A\varepsilon_0\varepsilon'(\omega)}{d} \tag{2}$$

where A is the electrode area, d the electrode separation distance and ε_0 the permittivity of free space. Similarly, the imaginary component of the permittivity $\varepsilon''(\omega)$ is related to the measured dielectric loss $G(\omega)/\omega$ of the system by:

$$\frac{G(\omega)}{\omega} = \frac{A\varepsilon_0\varepsilon''(\omega)}{d} \tag{3}$$

In an ideal system consisting of a single dipole embedded in a non-viscous medium, the dielectric response can be

described by Debye equation [14]

$$\varepsilon^*(\omega) = \varepsilon(\infty) + \chi(0)\frac{1}{1 + i\omega\tau} \quad (4)$$

where $\varepsilon(\infty)$ is the permittivity at infinite frequency, $\chi(0)$ is static susceptibility (i.e. the susceptibility as the frequency tends to zero) and τ is the relaxation time. A maximum is seen in the loss (imaginary) peak when $\omega = 1/\tau$. The dielectric response of the sample is therefore described by the two intrinsic parameters, $\chi(0)$ and τ, with the relaxation time being derived by mathematical inversion of the peak value of ω.

Most, if not all, real systems deviate to at least some extent from the Debye ideal and several mathematical treatments are available to interpret these deviations. These range from the essentially empirical [15–17] to the more theoretically based [18,19]. In our work, we have favoured the quantum mechanical approach developed by Dissado and Hill [19]. Essentially, the system under test is assumed to be composed of clusters of relaxing dipoles. Within each cluster, the dipoles will show cooperative behaviour during the relaxation process, and there may also be interaction between the clusters. Mathematically, the Dissado–Hill dielectric response is given by:

$$\varepsilon^*(\omega) = \varepsilon(\infty) + \frac{i\sigma_0}{\varepsilon_0\omega} + \chi(0)\frac{1}{(1 + i\omega\tau)^{n-1}} \, {}_2F_1\left(1 - n, 1 - m; 2 - n; \frac{1}{1 + i\omega\tau}\right) \quad (5)$$

In this case, a term to account for the direct current (dc) conductance apparent with aqueous samples has been included, i.e. σ_0.

${}_2F_1(,;;)$ is the Gaussian hypergeometric function given by

$${}_2F_1(a, b; c; z) = \sum_{n=0}^{\infty} \frac{(a)_n (b)_n}{(c)_n} \frac{(z)^n}{n!} \quad (6)$$

where

$$(a)_n = a(a + 1)(a + 2)\cdots(a + n - 2)(a + n - 1) \quad (7)$$

The indices n and m in Eq. (5) describe, respectively, the interactions within a cluster and the interactions between clusters. The value of n varies between 0 (no cooperation between dipoles in the cluster) and 1 (full cooperation). Similarly, a value of $m = 0$ indicates no interaction between neighbouring clusters, while $m = 1$ indicates full cooperation. Based on its theoretical derivation, m can also be regarded as being a descriptor of long-range homogeneity within a system, with $m = 0$ representing perfect equivalence of neighbouring clusters and $m = 1$ representing inhomogeneity between the clusters.

The dielectric response of the sample is therefore described by four intrinsic parameters: $\chi(0)$, τ, n and m. In practice, the experimental data are fitted to the Dissado–Hill equation using proprietary software to obtain values of these parameters. From there it is a trivial exercise to obtain the temperature dependence of the relaxation time by fitting the values of τ obtained at different temperatures to the relevant kinetic equation, e.g. Arrhenius or Vogel–Tammann–Fulcher.

3. Materials and methods

3.1. Materials

HSA Fraction V (published molecular weight 66,000) and PVP 29–32 (average molecular weight 40,000) were supplied by Sigma, MO, USA and were used as received. Purified water was generated using an Elga still (Elga, Bucks, UK). Aqueous solutions were prepared under ambient laboratory conditions using Class A volumetric glassware. Solutions were allowed to equilibrate for 2 h before being used. For the HSA alone, solutions of 1.0–10.0 w/v% concentration were prepared. For the combined HSA/PVP solutions, the concentration of each ingredient was varied from 1 to 5 w/v%.

3.2. MTDSC studies

MTDSC was performed using a TA Instruments model 2920 calorimeter. Helium was used as the carrier gas for all experiments due to its greater thermal conductivity at low temperatures than nitrogen. Matched hermetically sealed aluminium pans sourced from TA Instruments were used for all runs. Full calibration was performed before the acquisition of experimental data, using a scanning rate of 2 °C/min. Baseline calibration was performed using matched, empty pans. Temperature calibration runs were performed using *n*-octadecane (99.9%, Riedel-de-Hahn AG, Germany, theoretical melting point 28.24 °C), cyclohexane (99.9%, Riedel-de-Hahn AG, Germany, theoretical melting point 6.54 °C) and *n*-decane (99.9%, Riedel-de-Hahn AG, Germany, theoretical melting point −26.66 °C). Heat capacity constant calibration was performed using aluminium oxide (100 mesh, 99.9%, Aldrich Chemical Co., WI, USA). The sample and reference pans were loaded into the MTDSC cell at ambient temperature and the chamber sealed. The sample chamber was then held at 25 °C for 10 min, cooled at 2 °C/min to −60 °C, held at −60 °C for 10 min and heated at 2 °C/min to 40 °C, modulating the heat flow on the upward cycle with the following parameters: amplitude 0.2 °C; period 50 s, underlying heating rate 2 °C/min. Data were recorded on the heating cycle only. Two samples of each concentration of solution were studied, with sample sizes ranging from 10.5 to 19.5 mg. Excellent reproducibility was found between repeat runs.

3.3. Dielectric studies

Low frequency dielectric spectroscopy was performed using a BDC-N broadband dielectric converter

(Novocontrol GmbH, Germany) linked to a Frequency Response Analyser (Solartron—Schlumburger, Germany). The sample temperature was controlled to ±0.1 °C by the use of a Quatro temperature control system (Novocontrol GmbH, Germany). Parallel plate stainless steel electrodes of area 254.5 mm^2 and separation distance 0.5 mm were used, with an applied voltage of 0.5 V rms. Isothermal dielectric spectra were obtained over a frequency range of 10^6–10^{-2} Hz every 10 °C from 20 to −70 °C, with the sample temperature being reduced at 2 °C/min between measurements. Samples of purified water and each concentration of solution were studied at least in duplicate.

The real and imaginary components of the measured data in the frequency domain were fitted simultaneously to the Dissado–Hill equation using the Winfit 2.6 computer program (Novocontrol GmbH, Germany).

4. Results

4.1. MTDSC studies

A single melting transition at circa 0 °C was observed in the samples of frozen HSA solutions, corresponding to the melting of frozen water. No glass transitional behaviour was observed for any HSA solution over the temperature range accessible. Previous work has established that the T'_g of frozen PVP solutions is circa −19 °C [13,20], with the observed change in heat capacity (ΔC_p) increasing with increasing initial PVP concentration. Unfortunately, in the previous study it was not possible to precisely quantify the magnitude of ΔC_p at T_g due to interference from a pre-melting peak observed in the reversing heat flow signal, but the value was very small, particularly for the low initial concentrations of PVP such as 1 w/v%. Nevertheless, it was clearly demonstrated in both studies that the glass transition was detectable at this concentration level. For the mixed systems, solutions containing PVP in a greater molar concentration than HSA, e.g. PVP 5 w/v%:HSA 1 w/v%, showed a glass transition at circa −20 °C in both the total heat flow and reversing heat flow signals. However, in all other mixed samples, whereby the PVP was not in excess, no clear glass transition was observed. The relationship between the relative concentration of the two ingredients and thermal behaviour is therefore complex. Fig. 1 shows these results for representative samples.

4.2. Dielectric spectroscopy

In the liquid state, the HSA solutions and the mixed solutions of HSA and PVP showed dielectric spectra that were qualitatively similar to each other and to those previously reported for PVP solutions and purified water [13]. Fig. 2 shows the dielectric spectrum of a representative sample (2 w/v% HSA solution) and purified water at 20 °C. All samples exhibited a typical aqueous

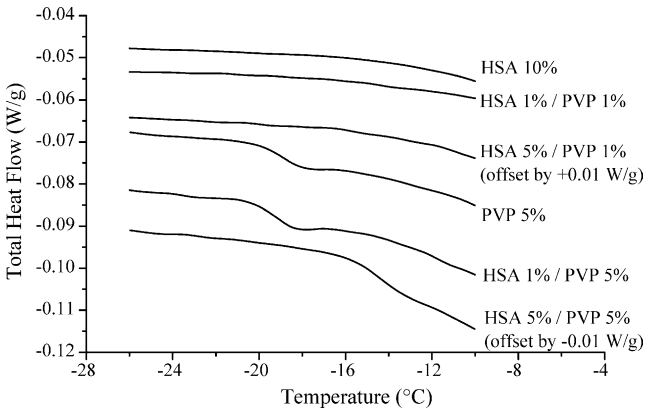

Fig. 1. The total heat flows of representative samples of HSA/PVP solutions in the area of the glass transition.

Maxwell–Wagner-type interfacial response, which corresponds electrically to the behaviour of two layers in series. Maxwell–Wagner behaviour has been described theoretically for dispersive media [21] and shown experimentally for several pharmaceutical systems [22,23]. For all samples, the log–log gradient of the high frequency dielectric loss was −1, indicating dc conductivity in the bulk region. This log–log gradient is equal to $(-1+n)$ in the Dissado–Hill notation and therefore corresponds to a value of 0 for the parameter n. Electrically, therefore, the dipoles behave independently, as would be expected for a simple bulk aqueous solution. All samples showed higher values for the dielectric loss in this region than did purified water alone, reflecting their greater conductivity. As would be expected from an ionisable material such as HSA, the values of the high frequency (bulk) capacitance and dielectric loss increased with increasing solution concentration, and were greater than those seen previously for the PVP solutions [13]. The values of the mixed solutions were intermediate between those of the individual solutions, but tended more towards those of the PVP solutions. The log–log gradients

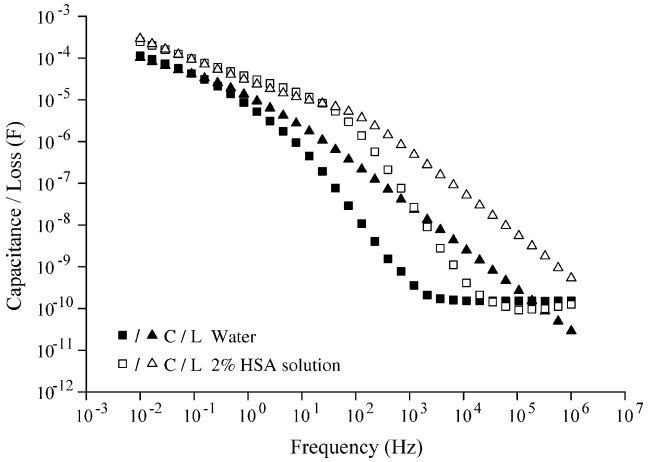

Fig. 2. The capacitance (C) and dielectric loss (L) of purified water and 2% HSA solution at +20 °C.

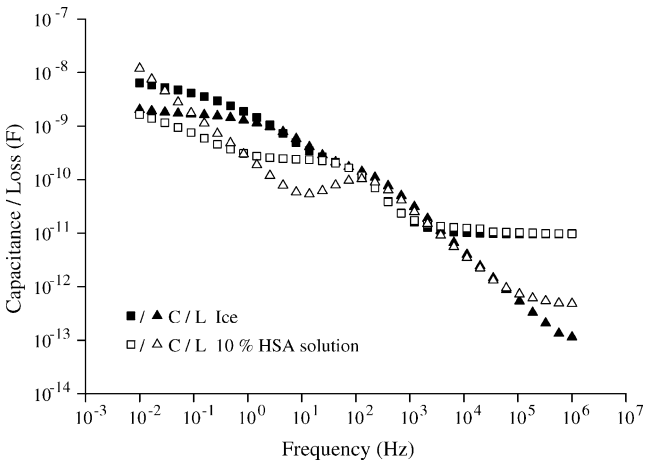

Fig. 3. The capacitance (C) and dielectric loss (L) of purified water and 10 w/v% HSA solution at −70 °C.

of both the capacitance and dielectric loss in the low frequency (barrier) region for all samples were circa −0.5, indicating that in this region charge migration occurs via a diffusion process.

In the frozen state, the response for ice shows a frequency-independent capacitance in the bulk region, corresponding to the 'static dielectric constant', and a diffusion process in the barrier region [13]. Although there was remarkable similarity in the responses of all of the HSA solutions in the frozen state, they showed a markedly different spectral shape to that of ice, as shown in Fig. 3 for the 10 w/v% solution and purified water at −70 °C. A Debye-type relaxation peak is clearly seen in the kHz region of the spectra of the frozen HSA solutions, with the characteristic peak maximum in the loss response and the step change in capacitance. At lower frequencies a further, essentially dc, conductivity is observed.

As the temperature of the HSA solutions is decreased, the peak loss maximum shifts to lower frequencies, indicating an increase in the relaxation time. The low frequency conductivity decreases as the temperature decreases,

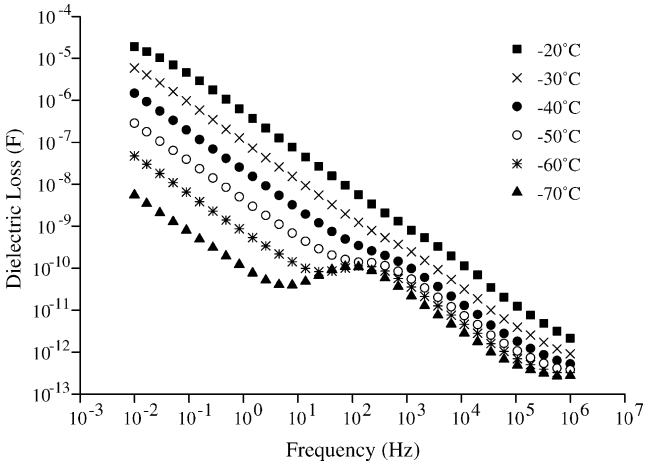

Fig. 4. The dielectric loss of 1 w/v% HSA solution at various temperatures in the frozen state.

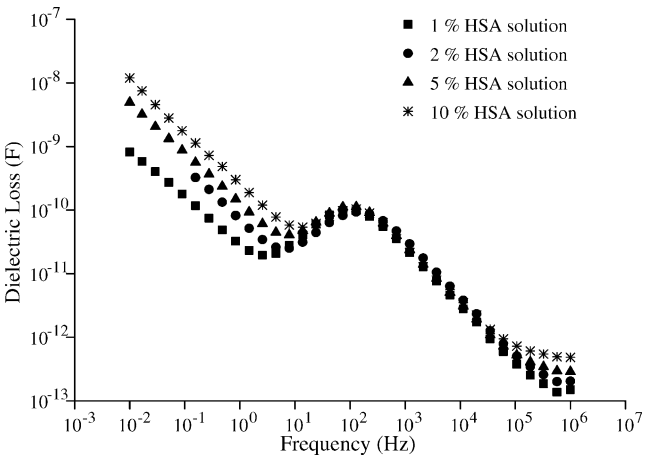

Fig. 5. The dielectric loss of frozen HSA solutions at −70 °C.

as would be expected due to the decreased mobility of the charges. This is shown in Fig. 4 for the 5 w/v% HSA solution. However, it is interesting to note that, for each temperature, the peak loss maximum shows very little variation with HSA concentration, as shown in Fig. 5 for a representative temperature of −70 °C.

The spectra of the frozen mixed solutions of HSA and PVP were qualitatively similar to those of the individual constituents, in that a Debye-type relaxation peak was observed in the kHz region of the spectra and that for each solution the peak loss maximum shifted to lower frequencies with decreasing temperature. Again, a further, essentially dc process was observed at very low frequencies. The peak loss frequency and the magnitude of the response of the mixed HSA/PVP solutions in the solid state appeared to vary in a complex fashion with composition, exemplified at a representative temperature of −70 °C in Fig. 6.

These results for the mixed solutions are in direct contrast to those for solutions of the individual components, where virtually no concentration-dependence of the loss peak (and hence relaxation time) was seen (see Ref. [13] for the PVP solutions and Fig. 5 for the HSA solutions). In the case of the mixed systems, the PVP appears to dominate

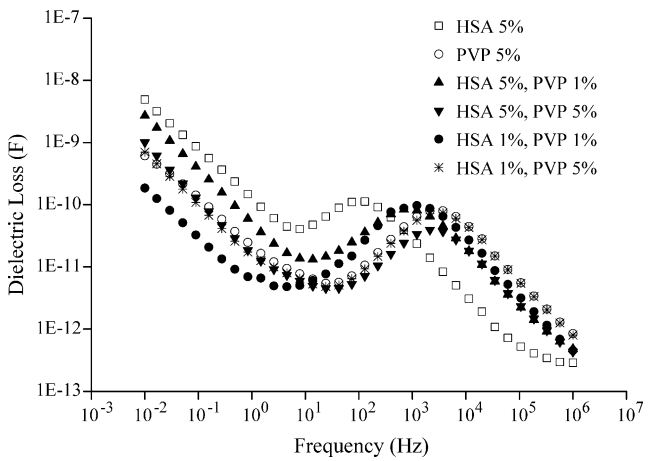

Fig. 6. The dielectric loss of frozen PVP/HSA solutions at −70 °C.

Table 1
The calculated relaxation times of frozen aqueous PVP, HSA and PVP/HSA solutions at various temperatures

Solution	Relaxation time (s) at various temperatures (°C)					
	−20	−30	−40	−50	−60	−70
1 w/v% PVP	2.728×10^{-5}	3.346×10^{-5}	4.188×10^{-5}	5.475×10^{-5}	7.559×10^{-5}	1.126×10^{-4}
5 w/v% PVP	1.227×10^{-5}	1.602×10^{-5}	1.854×10^{-5}	2.867×10^{-5}	4.139×10^{-5}	5.019×10^{-5}
10 w/v% PVP	1.152×10^{-5}	1.080×10^{-5}	1.306×10^{-5}	2.024×10^{-5}	3.023×10^{-5}	4.678×10^{-5}
1 w/v% HSA	7.085×10^{-5}	1.200×10^{-4}	2.737×10^{-4}	6.144×10^{-4}	1.143×10^{-3}	2.055×10^{-3}
2 w/v% HSA	6.600×10^{-5}	1.050×10^{-4}	2.454×10^{-4}	5.724×10^{-4}	8.876×10^{-4}	7.122×10^{-4}
5 w/v% HSA	1.600×10^{-4}	1.792×10^{-4}	5.366×10^{-4}	9.041×10^{-4}	7.622×10^{-4}	1.472×10^{-3}
10 w/v% HSA	1.330×10^{-4}	1.980×10^{-4}	2.716×10^{-4}	4.619×10^{-4}	8.175×10^{-4}	1.475×10^{-3}
1 w/v% HSA and 1 w/v% PVP	1.210×10^{-5}	2.208×10^{-5}	3.865×10^{-5}	5.315×10^{-5}	7.592×10^{-5}	1.248×10^{-4}
1 w/v% HSA and 2 w/v% PVP	8.618×10^{-6}	1.535×10^{-5}	2.470×10^{-5}	2.935×10^{-5}	4.602×10^{-5}	7.466×10^{-5}
1 w/v% HSA and 5 w/v% PVP	7.753×10^{-6}	1.136×10^{-5}	1.407×10^{-5}	1.825×10^{-5}	2.553×10^{-5}	4.714×10^{-5}
2 w/v% HSA and 1 w/v% PVP	9.810×10^{-6}	3.157×10^{-5}	4.592×10^{-5}	7.056×10^{-5}	8.086×10^{-5}	6.333×10^{-5}
2 w/v% HSA and 2 w/v% PVP	8.525×10^{-6}	1.548×10^{-5}	2.721×10^{-5}	3.770×10^{-5}	5.176×10^{-5}	4.071×10^{-5}
2 w/v% HSA and 5 w/v% PVP	5.248×10^{-6}	7.964×10^{-6}	1.099×10^{-5}	1.362×10^{-5}	2.199×10^{-5}	2.139×10^{-5}
5 w/v% HSA and 1 w/v% PVP	1.799×10^{-5}	2.763×10^{-5}	4.199×10^{-5}	7.752×10^{-5}	1.200×10^{-4}	1.691×10^{-4}
5 w/v% HSA and 2 w/v% PVP	1.774×10^{-5}	2.289×10^{-5}	3.939×10^{-5}	5.904×10^{-5}	9.040×10^{-5}	1.211×10^{-4}
5 w/v% HSA and 5 w/v% PVP	1.236×10^{-5}	1.304×10^{-5}	1.490×10^{-5}	2.206×10^{-5}	3.229×10^{-5}	5.227×10^{-5}

Data for PVP solutions discussed in Ref. [13].

the response, and it is particularly noticeable that at the 5 w/v% PVP level in the mixed systems, the response is very similar to that of the pure 5 w/v% PVP solution. Conversely, the HSA is exerting less of an influence in the mixed systems, as even when it is present at the 5 w/v% level, the responses of the mixed system are closer to that of the 5 w/v% PVP solution than the 5 w/v% HSA solution.

The relaxation time, τ, can be calculated for each sample at each temperature from the inverse of the loss peak frequency by fitting the experimental data with a one-component Dissado–Hill model [10]. The relaxation times thus derived for all solutions studied are listed in Table 1. For the frozen HSA solutions, the relaxation times increased from approximately 0.1 ms to approximately 1 ms as the temperature was decreased from −20 to −70 °C, but remained reasonably constant at each temperature for the four concentrations studied. A similar response was previously seen for the frozen PVP solutions [13], with the relaxation times for these solutions being approximately one order of magnitude shorter than those of the HSA solutions. The calculated relaxation times for the mixed systems varied with both temperature and concentration of the two ingredients, as would be inferred from Fig. 6.

The activation energies of the relaxation process can then be calculated by fitting the values of τ to the Arrhenius equation

$$\tau = A \exp(E_a/RT) \quad (9)$$

where A is the pre-exponential factor, E_a the activation energy, R is the gas constant and T is the temperature in Kelvin. Fig. 7 shows the Arrhenius plot of the derived relaxation times of representative frozen PVP/HSA solutions, with the fitted parameters being summarised in Table 2. The calculated activation energies ranged from 12.1 kJ/mol for the 1 w/v% PVP solution to 29.8 kJ/mol for the 1 w/v% HSA solution. Interestingly, the values of the activation energy for the PVP solutions showed a small increase with increasing initial concentration (to 13.1 kJ/mol for the 5 w/v% solution), whereas the converse was true of the HSA solutions, with the activation energy decreasing to 20.7 kJ/mol for the 10 w/v% solution. The values of the mixed solutions were intermediate between those of the corresponding individual component solutions. As observed earlier for the dielectric spectra themselves and the derived relaxation times, the PVP had a greater effect on the activation energies of the mixed systems than the HSA. Indeed, for all individual concentrations of HSA in the mixed systems, increasing the PVP concentration resulted in a decrease in the activation energy, such that the mixed solutions containing 5 w/v% PVP showed activation

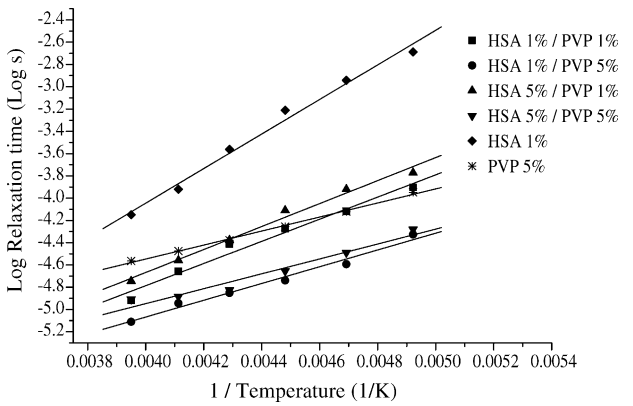

Fig. 7. The Arrhenius plot of the calculated relaxation times of representative frozen PVP/HSA solutions.

Table 2
The Arrhenius fitting parameters used to model the temperature dependence of the relaxation time of frozen aqueous PVP, HSA and PVP/HSA solutions

Solution	Pre-exponential factor (s)	Activation energy (kJ/mol)	Linear regression correlation coefficient
1 w/v% PVP	8.588×10^{-8}	12.05	0.998
5 w/v% PVP	3.037×10^{-8}	12.63	0.992
10 w/v% PVP	1.848×10^{-8}	13.08	0.969
1 w/v% HSA	5.429×10^{-11}	29.776	0.995
2 w/v% HSA	1.472×10^{-9}	23.015	0.935
5 w/v% HSA	1.767×10^{-8}	19.343	0.938
10 w/v% HSA	6.934×10^{-9}	20.678	0.998
1 w/v% HSA and 1 w/v% PVP	1.713×10^{-9}	19.050	0.987
1 w/v% HSA and 2 w/v% PVP	2.645×10^{-9}	17.364	0.988
1 w/v% HSA and 5 w/v% PVP	8.338×10^{-9}	14.413	0.991
2 w/v% HSA and 1 w/v% PVP	1.649×10^{-8}	14.774	0.824
2 w/v% HSA and 2 w/v% PVP	1.553×10^{-8}	13.979	0.896
2 w/v% HSA and 5 w/v% PVP	1.644×10^{-8}	12.434	0.968
5 w/v% HSA and 1 w/v% PVP	1.599×10^{-9}	19.759	0.994
5 w/v% HSA and 2 w/v% PVP	5.092×10^{-9}	17.211	0.993
5 w/v% HSA and 5 w/v% PVP	2.375×10^{-8}	12.813	0.977

Data for PVP solutions discussed in Ref. [13].

energies very similar to those of the pure 5 w/v% PVP solution.

5. Discussion

The data have indicated that HSA and PVP do not exhibit simple additivity or complete dominance of one or other component when present as mixtures in frozen aqueous solution, but that the observed behaviour shows a complex relationship with concentration of the two ingredients.

One possible explanation of the MTDSC data is that HSA and PVP exist in a stoichiometric complex in the frozen state, with any excess HSA or PVP being associated with non-frozen water in a separate phase. This phase-separated solution will then exhibit a glass transition (or not) depending on its chemical composition. The experimental data are compatible with the existence of a simple 1:2 HSA:PVP complex. For example, the system containing 1 w/v% PVP:1 w/v% HSA will lead to an excess of HSA on formation of the complex. Frozen 'pure' HSA solutions do not exhibit a glass transition in the temperature range accessible here and therefore none would be expected for this particular mixed system. Conversely, the system containing 5 w/v% PVP and 1 w/v% HSA will lead to an excess of PVP on formation of the complex. As 'pure' PVP solutions exhibit a glass transition at circa -20 °C, a similar glass transition would be expected for this sample. For all the concentrations studied here, the experimental data are compatible with the predictions from this model.

The results and interpretation presented here, i.e. the formation of 1:2 HSA:PVP complex and a separate solution phase containing the 'excess' PVP or HSA are in contrast to those of Izutsu and Kojima [24] who showed that solutions of PVP and three model proteins (bovine serum albumin, ovalbumin and chicken egg lysosyme), in similar concentrations to those studied here, remained compatible on freezing, forming a single amorphous phase as judged by DSC. However, as these authors themselves remarked, polymer–protein miscibility in the frozen state has not been well studied due to the paucity of suitable available techniques and further work is required to fully elucidate the fine structure of these systems on freezing.

The dielectric studies showed a clear relaxation peak for all the frozen systems studied. While such peaks represent the behaviour of the bulk system as a whole rather than individual components as such, it has previously been suggested that the relaxation in frozen PVP solutions is dominated by unfrozen water rather than by ice or PVP [13], based on comparisons with literature values of relaxation times and activation energies for water, ice and PVP. In the liquid state, water has been reported to have τ values in the region of 10 ps, while in the solid (ice) state the value increases to approximately 100 μs (i.e. within the same order of magnitude as reported here), this difference being due to the increased viscosity of the microenvironment surrounding each dipole in ice compared to that in unfrozen water [25]. Literature values of the activation energies for the dielectric relaxations of water and ice are 19 and 55 kJ/mol, respectively [25]. The corresponding value for PVP (mw 40,000) is 46.3 kJ/mol [26]. No equivalent data are available for HSA, but one may expect the activation energy of this material to be closer to that of PVP than water, based on molecular weight. By an extension of our previous argument, it is likely that the dielectric relaxation in HSA solutions is also dominated by unfrozen water.

The difference in the relaxation times of unfrozen water in HSA solutions and in PVP solutions may then be explained by local viscosity effects, with the effect of viscosity on the relaxation time being given by

$$\tau = \frac{4\pi a^3 \eta}{kT} \quad (10)$$

where a is the radius of the relaxing species, η is the viscosity of the immediate environment, k is the Boltzmann constant and T is the temperature in Kelvin [14].

If the radius of the relaxing dipole in water is taken as being 0.14 nm, approximately half the separation distance between two molecules in liquid water [27], then the values of the local viscosity surrounding the dipole of interest in this case are in the range 5×10^2–1×10^5 Pa s. Although this is significantly higher than the viscosity of liquid water under ambient conditions, e.g. 0.18 Pa s at 0 °C, it is several orders of magnitude lower than that of ice at 0 °C, 10^{13}–10^{15} Pa s. From the relaxation time data presented in Table 1, it can be inferred that the micro-viscosity around a water dipole in a frozen HSA solution is approximately one order of magnitude greater than that in a frozen PVP solution. Additionally, the rate of increase in viscosity with decreasing temperature varies between the two systems, with the frozen PVP solutions showing an approximately 3-fold increase in viscosity over the temperature range −20 to −70 °C and the frozen HSA solutions showing an approximately 8-fold increase over the same temperature range. The similarities in the dielectric spectra, relaxation times and activation energies between the frozen mixed HSA/PVP systems studied here and the single component systems indicate that the same relaxation process is occurring in all samples. Again, the relaxing species is postulated to be unfrozen water. As discussed above, local viscosity changes around individual dipoles in the different systems may account for the differences in relaxation time observed here. The variation in the local viscosity with changing HSA and PVP content indicates that these two compounds are interacting to some extent in the frozen systems, as would be inferred from the MTDSC studies. The precise nature of this interaction is unknown but as the overall effect of increasing PVP concentration whilst maintaining HSA concentration is to reduce the local viscosity, it may be postulated to be a form of crystallisation inhibition, i.e. the PVP may be preventing the crystallisation of ice that would normally occur during the freezing of a solution of HSA. Alternatively, as the MTDSC results indicated that the HSA and PVP may form a complex in the frozen state, leading to phase separation of an unfrozen solution of the solute present in excess, the variation in viscosity around the relaxing water dipole may be related to the variation in the excluded complex phase.

Examination of the values of the Dissado–Hill parameters n and m indicate that these parameters showed little variation with either concentration of the two ingredients or temperature, remaining at approximately $n = 0.1$ and $m = 0.8$ throughout. As indicated above, n is a measure of the cooperativity between dipoles and a low value of n indicates essentially dc conductivity as would be expected from unfrozen water. The high value of the parameter m indicates that there is extensive inhomogeneity throughout the system, as would be expected for an amorphous material. Hence, the cooperative factors n and m support the contention that it is the unfrozen water within the system that is being measured here.

These results are generically interesting because they suggest that dielectric spectroscopy may be a useful way of observing the behaviour of water in frozen multi-component systems, as this technique allows direct measurement of the relaxation time of water in the system. It is both conceptually and experimentally simple to manipulate the composition of the system and examine the effects of such formulation change on the relaxation behaviour of the water dipoles. By comparing the measured relaxation times of different formulations, the viscosity of the micro-environment surrounding the dipole may be determined. This in turn may be of use in determining the overall structure of the multi-component system and allow prediction of location of particular constituents and as assessment of the likely behaviour of the system. As the degradation of protein molecules during the freeze-drying process is thought to be related to water activity and as one theory of cryoprotection is that the protein exists in a shell of amorphous water [28], the ability to obtain information on the behaviour of water within the system may be of considerable importance in the development of freeze-dried products. Indeed, the implication from these results that the PVP alters the aqueous microenvironment in which the HSA is located may have relevance to the manner in which this and other cryoprotectants exert their action.

6. Conclusions

MTDSC and dielectric spectroscopy in combination are of use in the study of frozen amorphous systems, with the two techniques examining different facets of the behaviour of these systems. MTDSC allows examination of the gross, cooperative molecular mobility of the amorphous system as a whole and allows examination of the effect of co-mixing on the heat capacity change through T_g. Dielectric spectroscopy investigates the relaxation behaviour in amorphous systems, as the response allows clear visualisation of frequency dependent dipolar relaxation processes following excitation by the electrical stimulus. The relaxation time may be calculated simply from the inverse of the frequency corresponding to the maximum in the imaginary permittivity. The data suggest that the relaxation behaviour is an indication of the molecular mobility of the unfrozen water fraction within the system, in turn implying that these techniques may be a useful means of developing our understanding of the mode of action of cryoprotectants.

References

[1] F. Franks, Freeze drying: from empiricism to predictability, Cryo-Letters 11 (1990) 93–110.

[2] F. Franks, Freeze-drying of bioproducts: putting principles into practice, Eur. J. Pharm. Biopharm. 45 (1998) 221–229.

[3] J.F. Carpenter, M.J. Pikal, B.S. Chang, T.W. Randolph, Rational design of stable lyophilized protein formulations: some practical advice, Pharm. Res. 14 (1997) 969–975.

[4] H. Levine, L. Slade, Thermomechanical properties of small carbohydrate–water glasses and rubbers—kinetically metastable systems at subzero temperatures, J. Chem. Soc., Farad. Trans. 84 (1988) 2619–2633.

[5] T.W. Randolph, Phase separation of excipients during lyophilisation: effects on protein stability, J. Pharm. Sci. 86 (1997) 1198–1203.

[6] S.P. Duddu, G. Zhang, P.R. Dal Monte, The relationship between protein aggregation and molecular mobility below the glass transition temperature of lyophilized formulations containing a monoclonal antibody, Pharm. Res. 14 (1997) 596–600.

[7] S.L. Shamblin, X. Tang, L. Chang, B.C. Hancock, M.K. Pikal, Characterisation of the time scales of molecular motion in pharmaceutically important glasses, J. Phys. Chem. B 103 (1999) 4113–4121.

[8] B.C. Hancock, S.L. Shamblin, G. Zografi, Molecular mobility of amorphous pharmaceutical solids below their glass-transition temperatures, Pharm. Res. 12 (1995) 799–806.

[9] V. Andronis, G. Zografi, Molecular mobility of supercooled amorphous indomethacin, determined by dynamic mechanical analysis, Pharm. Res. 14 (1997) 410–414.

[10] M.J. Pikal, Freeze drying of proteins, in: J.L. Cleland, R. Langer (Eds.), Formulation and delivery of proteins and peptides, ACS Symposium Series 567, American Chemical Society, Washington, 1993.

[11] R. Okada, S. Matsukawa, T. Watanabe, Hydration structure and dynamics in pullulan aqueous solution based on H-1 NMR relaxation time, J. Mol. Struct. 602 (2002) 473–483.

[12] D. Le Botlan, J. Wennington, J.C. Cheftel, Study of the state of water and oil in frozen emulsions using time domain NMR, J. Colloid Interface Sci. 226 (2000) 16–21.

[13] S.A. Barker, R. He, D.Q.M. Craig, Low frequency dielectric investigations into the relaxation behaviour of frozen polyvinylpyrrolidone–water systems, J. Pharm. Sci. 90 (2001) 157–164.

[14] P. Debye, Polar Molecules, Dover Publications, London, 1945.

[15] K.S. Cole, R.H. Cole, Dispersion and absorption in dielectrics, J. Chem. Phys. 9 (1941) 341–351.

[16] D.W. Davidson, R.H. Cole, Dielectric relaxation in glycerol, propylene glycol and *n*-propanol, J. Chem. Phys. 19 (1951) 1484–1490.

[17] S. Havriliak, S. Negami, A complex plane analysis of α-dispersions in some polymer systems, J. Polym. Sci., Part C 14 (1966) 99–117.

[18] A.K. Jonscher, A new model of dielectric loss in polymers, Colloid Polym. Sci. 253 (1975) 231–250.

[19] L.A. Dissado, R.M. Hill, Non-exponential decay in dielectrics as a consequence of the dynamics of correlated systems, Nature 279 (1979) 685–689.

[20] L.-H. Her, S.L. Nail, Measurement of glass transition temperatures of freeze-concentrated solutes by differential scanning calorimetry, Pharm. Res. 11 (1994) 54–59.

[21] R.M. Hill, C. Pickup, Barrier effects in dispersive media, J. Mater. Sci. 20 (1985) 4431–4444.

[22] J. Binns, D.Q.M. Craig, R.M. Hill, M. Davies, C. Melia, J.M. Newton, Dielectric characterisation of sodium alginate gels, J. Mater. Chem. 2 (1992) 545–549.

[23] S.A. Barker, D.Q.M. Craig, K.M.G. Taylor, R.M. Hill, An investigation into the low frequency dielectric response of liposomes, J. Colloid Interface Sci. 166 (1994) 66–72.

[24] K. Izutsu, S. Kojima, Freeze-concentration separates proteins and polymer excipients into different amorphous phases, Pharm. Res. 17 (2000) 1316–1322.

[25] J.B. Hasted, Aqueous Dielectrics, Chapman & Hall, London, 1973.

[26] S.K. Jain, G.P. Johari, Dielectric studies of molecular motions in the glassy states of pure and aqueous poly(vinylpyrrolidone), J. Phys. Chem. 92 (1988) 5851–5854.

[27] E.H. Grant, R.J. Sheppard, G.P. South, Dielectric Behaviour of Biological Molecules in Solution, Clarendon Press, Oxford, 1978.

[28] D.Q.M. Craig, P.G. Royall, V.L. Kett, M.L. Hopton, The relevance of the amorphous state to pharmaceutical dosage forms: glassy drugs and freeze dried systems, Int. J. Pharm. 179 (1999) 179–207.